Crystallographic Evidence of Drastic Conformational Changes in the Active Site of a Flavin-Dependent N-Hydroxylase

BIOCHEMISTRY
including biophysical chemistry & molecular biology

Article

pubs.acs.org/biochemistry

Crystallographic Evidence of Drastic Conformational Changes in the Active Site of a Flavin-Dependent *N*-Hydroxylase

Jeremy W. Setser,[†] John R. Heemstra, Jr.,[∥,⊥] Christopher T. Walsh,[∥] and Catherine L. Drennan*[,†,‡,§]

[†]Department of Chemistry, [‡]Department of Biology, and [§]Howard Hughes Medical Institute, Massachusetts Institute of Technology, 77 Massachusetts Avenue, Cambridge, Massachusetts 02139, United States

[∥]Department of Biological Chemistry and Molecular Pharmacology, Harvard Medical School, 240 Longwood Avenue, Boston, Massachusetts 02115, United States

Supporting Information

ABSTRACT: The soil actinomycete *Kutzneria* sp. 744 produces a class of highly decorated hexadepsipeptides, which represent a new chemical scaffold that has both antimicrobial and antifungal properties. These natural products, known as kutznerides, are created via nonribosomal peptide synthesis using various derivatized amino acids. The piperazic acid moiety contained in the kutzneride scaffold, which is vital for its antibiotic activity, has been shown to derive from the hydroxylated product of L-ornithine, L-N^5-hydroxyornithine. The production of this hydroxylated species is catalyzed by the action of an FAD- and NAD(P)H-dependent *N*-hydroxylase known as KtzI. We have been able to structurally characterize KtzI in several states along its catalytic trajectory, and by pairing these snapshots with the biochemical and structural data already available for this enzyme class, we propose a structurally based reaction mechanism that includes novel conformational changes of both the protein backbone and the flavin cofactor. Further, we were able to recapitulate these conformational changes in the protein crystal, displaying their chemical competence. Our series of structures, with corroborating biochemical and spectroscopic data collected by us and others, affords mechanistic insight into this relatively new class of flavin-dependent hydroxylases and adds another layer to the complexity of flavoenzymes.

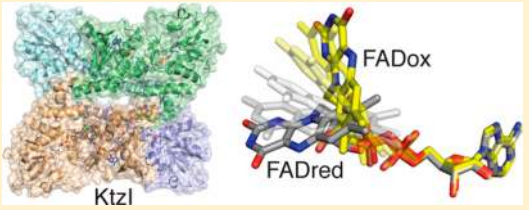

Natural products and their derivatives are vital for human health, as they comprise more than one-third of all Food and Drug Administration-approved small molecule drugs.[1] Many of these compounds are antibiotics that are biosynthesized by microbes via nonribosomal peptide synthesis (NRPS) pathways.[2] NRPS pathways are designed such that various enzymes act in an assembly line fashion to build up peptide chains using a broad range of both canonical and derivatized amino acids. Even with the chemical diversity present in currently available antibiotics, which is largely generated from the variety of permutations available in NRPS and similar systems, there exists a pressing need for new therapeutic candidates to combat drug-resistant infections.[2] Therefore, finding new molecular scaffolds with therapeutic benefit, and elucidating the biosynthetic pathways necessary to construct such compounds, is increasingly important.

Kutznerides make up a recently discovered class of antifungal antimicrobials produced by the soil actinomycete *Kutzneria* sp. 744.[3,4] These natural products are highly decorated, cyclic hexadepsipeptides (Figure 1a), which are constructed via NRPS. The gene cluster encoding this NRPS pathway has been elucidated,[5] and the functions of many of its biosynthetic components have been demonstrated *in vitro*.[5−11] One of these enzymes, KtzI, was originally annotated as a 47 kDa flavin-dependent lysine/ornithine *N*-monooxygenase (hydroxylase),[5] and this proposed activity was further investigated biochemically.[7]

KtzI was found to use a noncovalently bound FAD cofactor, reducing equivalents from NADPH or NADH (albeit less efficiently), and molecular oxygen to install a hydroxyl group on the side chain nitrogen of L-ornithine (L-Orn), producing L-N^5-hydroxyornithine (Figure 1b). Binding of substrate analogue L-lysine causes oxidation of the NADPH cofactor, without subsequent production of hydroxylysine, effectively uncoupling the reaction.[7] This specificity for the substrate, and the cofactor and cosubstrate usage, is similar to that of previously characterized flavin *N*-hydroxylases.[12−23] However, KtzI does differ from these other systems in the fate of its hydroxylated product.

The hydroxyornithine product of KtzI is ultimately incorporated into the kutzneride scaffold as the N−N bond-containing piperazic acid moiety[7] (Figure 1), which has been shown to be crucial for the antibiotic activity of these molecules.[3] The intramolecular cyclization necessary to reach this final structure, which is the creation of a bond between N^2 and N^5 of hydroxyornithine, is likely preceded by some further activation of the hydroxylamine, but no candidate enzymes have yet been established. In any case, the hydroxylation catalyzed by KtzI is not retained in the final piperazic acid product and thus is known as a "cryptic" modification. This use

Received: May 28, 2014
Revised: August 31, 2014
Published: September 3, 2014

   dx.doi.org/10.1021/bi500655q | *Biochemistry* 2014, 53, 6063−6077

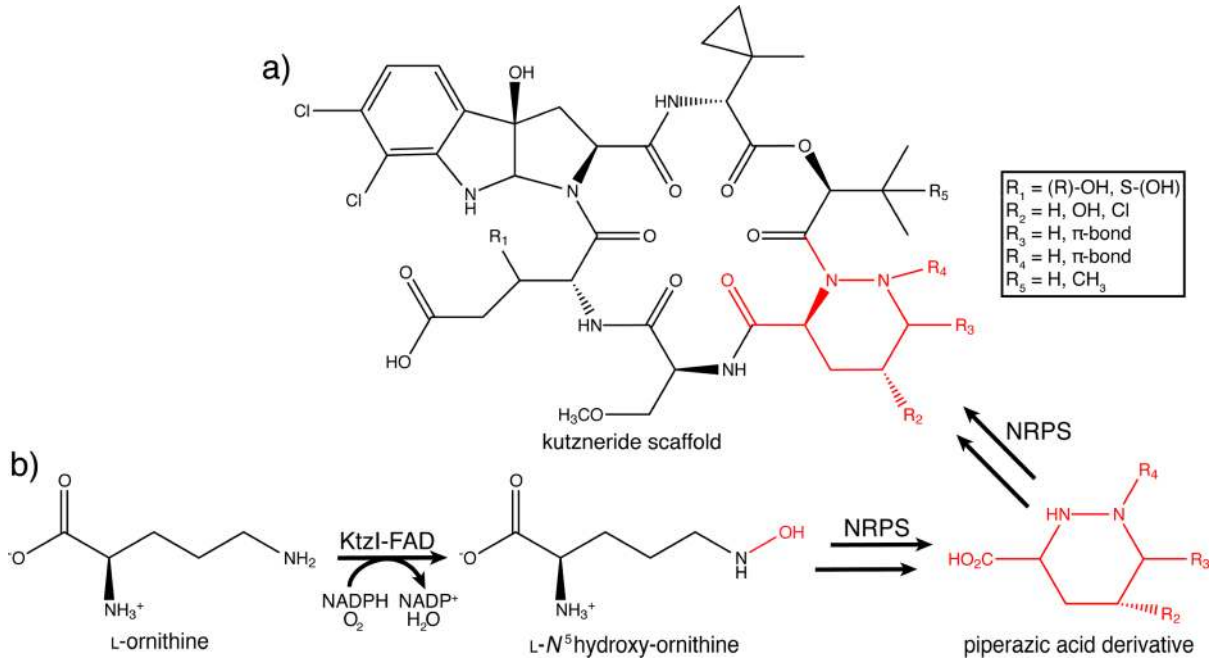

Figure 1. Kutzneride scaffold cryptically incorporates the product of KtzI. (a) The kutzneride hexadepsipetides are highly decorated natural products produced by nonribosomal peptide synthesis (NRPS). The piperazic acid moiety (red) of this scaffold is derived from the L-N^5-hydroxyornithine produced by KtzI. (b) KtzI uses FAD, NADPH, and O_2 to catalyze the production of its hydroxy product from L-ornithine (-OH colored red), which is further processed and inserted into the kutzneride scaffold by downstream enzymes.

of cryptic N-hydroxylation for antibiotic biosynthesis is a departure from the previously characterized members of the *N*-hydroxylase family. All other lysine and ornithine *N*-hydroxylases investigated to date have their hydroxy modifications carried on to the final product, where these moieties are used as ligands in iron-scavenging molecules called siderophores.[12−23] This divergence in the overall role of the N-hydroxylating protein has no observable effect on the chemistry involved, however, as these enzymes all catalyze the creation of a primary hydroxylamine product.

KtzI shares a high level of sequence homology (33% identical) with the L-Orn *N*-hydroxylases from *Pseudomonas aeruginosa* (PvdA) and *Aspergillus fumigatus* (SidA) (Figure S1 of the Supporting Information), which have been characterized in detail both biochemically[15−17,20,21,24−28] and structurally.[29,30] In the biochemical studies, PvdA and SidA were proposed to follow a similar reaction mechanism as outlined in Figure 2. Common to most flavin monooxygenases, the oxidized FAD cofactor is reduced by hydride transfer from the C4-*pro-R* position of the NADPH nicotinamide to the N^5 position of the flavin isoalloxazine ring, completing what is known as the reductive half of the reaction (Figure 2, **1** → **3**). The oxidative half of the reaction begins when molecular oxygen adds to the reduced flavin species, creating the highly reactive C4a-(hydro)peroxy intermediate (Figure 2, **4b** and **5**). Hydroxylation occurs through nucleophilic attack by the bound substrate (here the side chain amine of L-Orn) on the activated flavin−hydroperoxide intermediate, producing both the hydroxylated product and a hydroxy-FAD intermediate (Figure 2, **5** → **6**). The oxidized flavin species is regenerated through the loss of water, and that with the concomitant dissociation of end products completes the catalytic cycle (Figure 2, **6** → **1**). If the hydroperoxy−flavin intermediate is not sufficiently protected or used improperly, it is lost as the toxic byproduct hydrogen peroxide, thus uncoupling the reductive and oxidative halves of the reaction and wasting the reducing equivalents provided by NADPH (Figure 2, "uncoupling"). Even though the *N*-hydroxylases follow this canonical mechanism, they diverge in other specifics and create what is effectively a hybrid between two flavin monooxygenase archetypes known as "cautious" and "bold" monooxygenases.

The "cautious" (or class A) monooxygenases, which are typified by the extensively studied *p*-hydroxybenzoate hydroxylase (PHBH) (reviewed in refs 31−33), have a stringent substrate specificity and also maintain tight regulation over the reductive half of their reaction cycle (Figure 2, **1** → **3**). In these enzymes, the rate of FAD reduction is intimately linked to substrate binding, such that the presence of the hydroxylatable target greatly enhances the reaction rate, upward of 10^5-fold for PHBH.[34] This control point significantly decreases the risk of uncoupling (Figure 2, "uncoupling"), as the addition of O_2 to reduced flavin, yielding the highly reactive C4a-hydroxperoxyflavin (Figure 2, **4b** and **5**), can occur only when the substrate is present to accept its hydroxy modification. On the other hand, in "bold" (or class B) monooxygenases, such as those of the Baeyer−Villiger monooxygenase (BVMO) and flavin monooxygenase (FMO) enzyme families, the reduction of FAD by NADPH occurs just as well with or without bound substrate, and thus, they must utilize a completely different tact to protect against uncoupling. In these systems, the spent $NADP^+$ cofactor remains bound to the protein throughout the reaction cycle, protecting both the reduced and the C4a-(hydro)peroxyflavin species from being quenched (reviewed in refs 31 and 32). "Bold" monooxygenases also tend to have little substrate specificity, illustrated by the more than 200 known compounds that the mammalian FMOs will hydroxylate.[35]

The *N*-monooxygenases, although formally grouped with the class B monooxygenases,[32] have been found to carry traits from both classes described above. They have the narrow substrate specificity of the "cautious" enzymes but show no sign of

dx.doi.org/10.1021/bi500655q | *Biochemistry* 2014, 53, 6063−6077

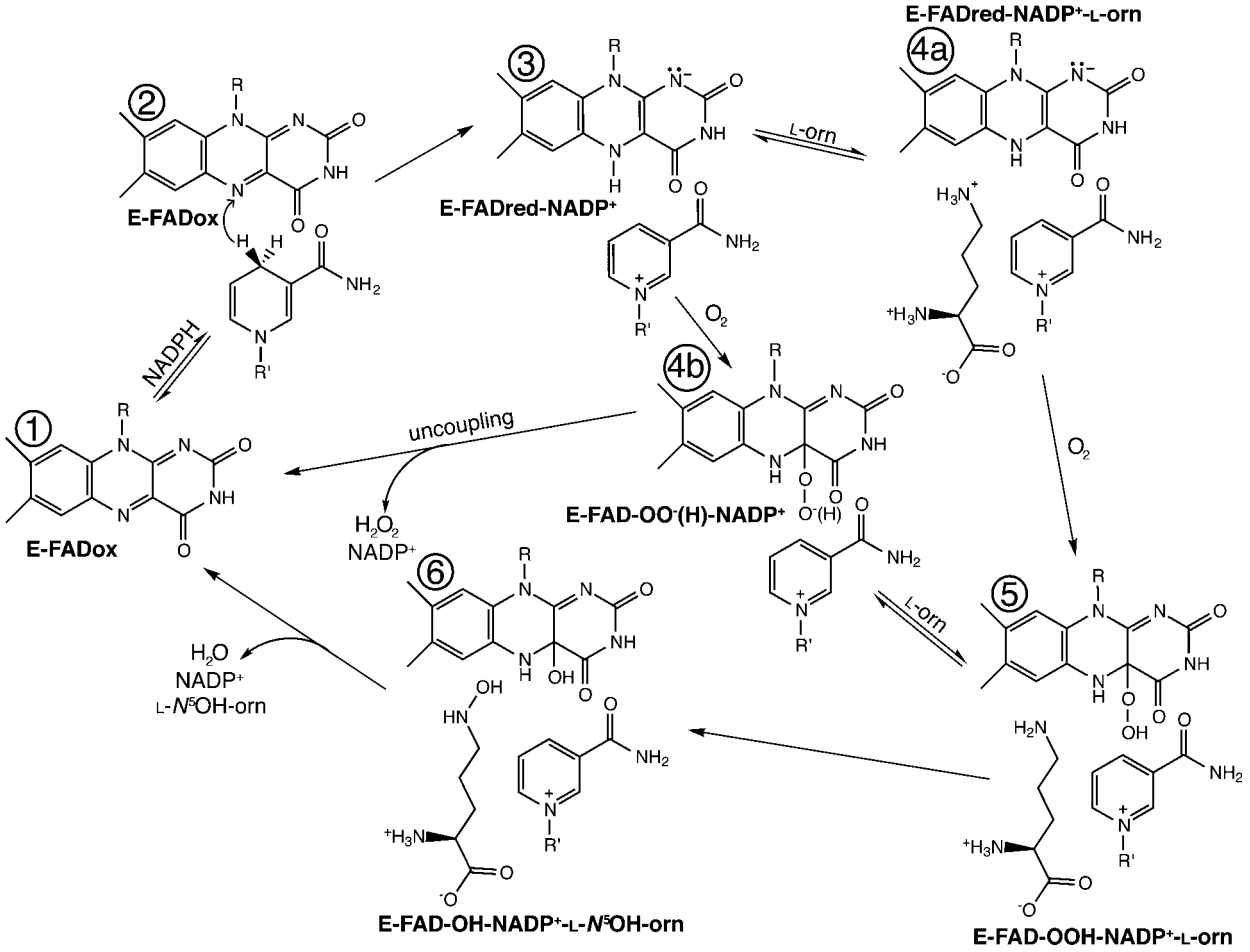

Figure 2. Proposed reaction mechanism for L-Orn *N*-hydroxylases. The flavin and nicotinamide cofactors are truncated to their reactive portions, and the schematic abbreviations are as follows: E, enzyme; FADox, oxidized FAD; FADred, reduced FAD; FAD-OO$^-$(H), (hydro)peroxyflavin; FAD-OH, hydroxyflavin; L-Orn, L-ornithine; L-N^5OH-Orn, L-N^5-hydroxyornithine. There is biochemical evidence to suggest that the L-Orn substrate binds with a protonated side chain amine[24] (**4a**), but the neutral form is eventually necessary for catalysis to occur, as it is used to attack the flavin–hydroperoxide intermediate to generate the hydroxyornithine product (**5** → **6**).

substrate-assisted reduction of FAD and remain bound to NADP$^+$ throughout catalysis,[15−17] which are both fundamental characteristics of "bold" monooxygenases. Structural insight into how catalysis is controlled by these hybrid monooxygenases has been provided by a series of recent crystal structures,[29,30] which describe how cofactors and substrate are bound in the active site. In this study, we build upon this structural knowledge by characterizing the *N*-hydroxylase KtzI in never-before-seen states of this enzyme class, including the anaerobically reconstituted, "preturnover" complex, and a view of the oxidized enzyme that suggests a drastic conformational change, with a novel flavin movement, takes place. The relevance of these unexpected conformational changes to catalysis is discussed.

MATERIALS AND METHODS

Protein Expression and Purification. The *ktzI* gene was cloned into a pET28a vector (Novagen), and the resulting N-terminal hexahistidine construct was transformed into BL21-(DE3) cells (Invitrogen) as described previously.[7] For protein overproduction, Luria-Bertani medium (LB) (100 mL supplemented with 50 μg/mL kanamycin) was inoculated using a glycerol stock of the expression strain and grown overnight at 30 °C and 200 rpm. Four 1 L cultures of LB containing 50 μg/mL kanamycin were each inoculated with 20 mL of the overnight culture and incubated at 25 °C and 200 rpm until the OD_{600} reached 0.5−0.6, at which point protein expression was induced by the addition of 100 μM IPTG. The cells were grown for 16 h postinduction at 15 °C and 200 rpm and harvested by centrifugation (6000*g* for 10 min). Cells were resuspended in lysis buffer [25 mM Tris-HCl (pH 8.0) and 500 mM NaCl] and lysed by sonication. The lysate was clarified by centrifugation (75000*g* for 35 min) and incubated with 5 mL of Ni-NTA slurry that had been pre-equilibrated in lysis buffer. This mixture was agitated at 4 °C for 1 h before being loaded into a column for purification. The resin was washed with lysis buffer supplemented with 0 mM (60 mL), 5 mM (60 mL), and 25 mM (60 mL) imidazole. KtzI was eluted with lysis buffer containing 200 mM (10 mL) and 500 mM (5 mL) imidazole, and the resulting eluate was concentrated to ∼1 mL in a 10K molecular weight cutoff (MWCO) filter (Millipore) by centrifugation (4500*g* for 10 min intervals). The concentrated sample was dialyzed against protein storage buffer [20 mM Tris-HCl (pH 8.0), 80 mM NaCl, and 10% (v/v) glycerol] in a 10K MWCO dialysis cassette (Thermo Scientific) over a period of 16 h with three buffer exchanges. The dialyzed protein solution (∼20 mg/mL by UV absorption at 280 nm; ε_{calc} = 48485 M^{-1} cm^{-1}) was flash-frozen in liquid nitrogen in 15 μL

dx.doi.org/10.1021/bi500655q | *Biochemistry* 2014, 53, 6063−6077

aliquots and stored at −80 °C. The final KtzI protein construct has 21 non-native amino acids (including the hexahistidine tag) at its N-terminus, followed by the wild-type sequence beginning with a valine residue at position 3 (Val3) (Figure S1 of the Supporting Information).

Reconstitution of KtzI for Crystallization. KtzI (10 mg/mL or ∼212 μM) was reconstituted with FAD (212 μM) and NADPH (4.24 mM) for all crystallization trials. To obtain substrate-bound structures, L-ornithine (31.8 mM) was added to this mixture. FAD, NADPH, and L-ornithine (all from Sigma-Aldrich) were diluted such that the final buffer composition of the reconstituted sample prior to crystallization included 20 mM Tris-HCl (pH 8.0), 80 mM NaCl, and 5% (v/v) glycerol. For anaerobic reconstitution, frozen tubes of KtzI protein and aliquots of FAD, NADPH, and L-ornithine powder were degassed and brought into an anaerobic chamber [95% argon and 5% hydrogen (COY Laboratory Products, Inc.)] prior to dilution with anaerobic buffer. All solutions for anaerobic manipulations had argon bubbled through them to remove oxygen. The final reconstituted samples were incubated in a cold block (∼4 °C) for 1 h before crystallization. Under anaerobic conditions, the characteristic color change from oxidized (FADox, yellow) to reduced (FADred, colorless) flavin could be observed in the sample, indicating hydride transfer from NADPH to FAD had occurred.

Crystallization of KtzI. Initial crystallization conditions were found using the Phoenix Liquid Handling System (Art Robbins Instruments) to mix 150 nL of reconstituted protein with 150 nL of precipitant in a 96-well, sitting-drop INTELLI-PLATE (Art Robbins Instruments) format. Crystals of reconstituted KtzI were optimized using the hanging-drop vapor diffusion method at room temperature by mixing 1 μL of reconstituted protein [containing 212 μM N-His_6-tagged protein, 212 μM FAD, 4.24 mM NADPH, (31.8 mM L-ornithine for substrate-bound structures), 20 mM Tris-HCl (pH 8.0), 80 mM NaCl, and 5% (v/v) glycerol] with 1 μL of precipitant over a reservoir of 0.5 mL of precipitant. KtzI crystallized with two precipitants: one of which afforded substrate binding [0.4−0.7 M (aerobic) or 0.9−1.15 M (anaerobic) KSCN, 22−25% PEG 3350, and 0.1 M Bis-tris propane (pH 8.5)] and the other precluding substrate binding because of a competing bromide ion [0.9−1.2 M (aerobic) or 1.2−1.4 M (anaerobic) NaBr, 22−25% PEG 3350, and 0.1 M Bis-tris propane (pH 7.5)]. Data-quality crystals grew as colorless [anaerobic (Figure S2a of the Supporting Information)] or yellow [aerobic (Figure S2b,c of the Supporting Information)] rods after 4−7 days with approximate dimensions of 70 μm × 70 μm × 200 μm. Crystals were cryoprotected with crystallization precipitant supplemented with 10−20% (v/v) glycerol (and with 31.8 mM L-Orn to ensure full substrate occupancy in the KtzI−FADred−$NADP^+$−L-Orn structure) before being flash-frozen in liquid nitrogen prior to data collection.

Re-reduction of Oxidized KtzI Crystals. To prepare re-reduced crystals, KtzI was first reconstituted with FAD and NADPH and crystallized aerobically under conditions that included NaBr as described above. After the formation of data-quality crystals, the crystallization tray was degassed and left under light vacuum overnight. The next day, the tray was degassed again and brought into the anaerobic chamber. Aliquots of NADPH and sodium dithionite powder were degassed, brought into the anaerobic chamber, and mixed with anaerobic crystallization precipitant to final concentrations of 50 and 25 mM, respectively.

The reduction of oxidized crystals was achieved by the addition of 4 μL of either the NADPH or sodium dithionite solution directly to the crystallization drop. Reduction was monitored visually as a color change from yellow to colorless. Both reductants were capable of eliciting this oxidation state change, but on very different time scales: 30 min for 50 mM NADPH and <10 s for 25 mM sodium dithionite. After reduction was complete, 4 μL of precipitant supplemented with 10% (v/v) glycerol was added to the drop for cryoprotection and crystals were looped and flash-frozen in liquid nitrogen. Soaking the crystals for 30 min in the 50 mM NADPH solution degraded them such that usable data could not be collected. Attempts to perform this same re-reduction protocol on crystals derived from KSCN-containing conditions proved to be unsuccessful, as evidenced by a complete lack of change in crystal color even during long incubation periods (5−10 min) with either reductant, culminating in the crystals dissolving into solution.

Reoxidation of Reduced KtzI Crystals. To prepare reoxidized crystals, KtzI was reconstituted with FAD, NADPH, and L-ornithine and crystallized anaerobically under conditions that included KSCN as described above. Once data-quality crystals formed, the crystallization tray was removed from the anaerobic chamber, and the change in oxidation state could be observed visually as crystals turned from colorless to yellow over a period of ∼1 h. The crystals were allowed to further equilibrate for ∼1 day before being cryoprotected and frozen in liquid nitrogen. Various attempts to partially oxidize these reduced crystals, in an effort to capture the C4a-hydroperoxy (or some other) intermediate state, were unsuccessful and resulted in either the reduced or oxidized equilibrium state described herein.

Data Collection, Structure Determination, and Structural Analysis. X-ray diffraction data were collected at the Advanced Photon Source (Argonne, IL) on beamline 24 ID-C and processed in space group $P2_12_12_1$ using HKL2000[36] (Tables S1−S6 of the Supporting Information). The initial structure of KtzI (reconstituted with FAD and NADPH anaerobically and crystallized under conditions that included NaBr) was determined by molecular replacement (MR) in PHASER[37] with a CHAINSAW[38] constructed search model using the protein coordinates of the *N*-hydroxylase from *P. aeruginosa*, PvdA (PDB entry 3S5W[30]), aligned with the sequence of KtzI. This hybrid model was created such that any conserved residues between PvdA and KtzI were retained, while all other residues were truncated to their last common atom according to the protein sequence of KtzI. Solvent content analysis suggested that four molecules of KtzI would occupy the asymmetric unit, and after using MR to search for four copies of the hybrid model, a homotetrameric assembly with extensive protein−protein interfaces was identified. All subsequent structures of KtzI, which adopted the same crystal packing, were determined by either MR or rigid body refinement in Refmac[39] using the initial refined model's protein coordinates. For rigid body refinements, the selection of reflections for the calculation of R_{free} was made identical in each model. Each KtzI structure has been abbreviated to signify what is bound to the protein, and the predicted oxidation states of the cofactors. The abbreviations used for these bound entities are as follows: FADred (reduced FAD), FADox (oxidized FAD), FADox-red (re-reduced FAD), FADred-ox (reoxidized FAD), $NADP^+$

Table 1. Summary of KtzI Structures

structure	resolution (Å)	Figures	FAD position	enzyme state	PDB entry
KtzI–FADred–$NADP^+$–L-Orn	2.23	3b,e and S7a	in	reduced preturnover with substrate	4TLX
KtzI–FADred–$NADP^+$–Br	2.39	S5a and S7b	in	reduced preturnover	4TM1
KtzI–FADox–Br	2.09	3c,f, S6a, and S7d	out	oxidized chemically competent	4TM3
KtzI–FADox–$NADP^+$–L-Orn	2.41	3d,g and S7e	out	oxidized dead end	4TLZ
KtzI–FADox-red–$NADP^+$–Br	2.63	S5d and S7c	out to in	re-reduced from KtzI–FADox–Br	4TM4
KtzI–FADred-ox–$NADP^+$–L-Orn	2.74	S6b and S7f	in to out	reoxidized from KtzI–FADred–$NADP^+$–L-Orn	4TM0

(oxidized NADP), L-Orn (L-ornithine), and Br (bromide ion that occupies the L-Orn binding pocket).

Files for describing ligand geometries were obtained in COOT,[40] which uses the REFMAC5 monomer library,[41] and included FDA (FADred), FAD (FADox), NAP (NADP), and ORN (L-ornithine). The restraints for these ligands were constructed using eLBOW, and those for FAD/FDA were further modified in REEL[42] from the PHENIX suite[43] to allow the flavin isoalloxazine ring to adopt its bent or "butterfly" conformation. This change was made such that the ring could fit the nonplanar electron density observed in our structures (Figure S3 of the Supporting Information). The modification of the flavin restraints involved dividing the isoalloxazine into two planes, or "wings", such that the dimethylbenzene and pyrimidine portions were restrained on separate planes, with each of these planes including the N^5 and N^{10} positions of the central pyrazine ring. The pyrazine ring, however, was not restrained to be planar, which allows bending of the outer "wings" of the isoalloxazine about the central N^5–N^{10} axis (Figure S3 of the Supporting Information). Ligand fitting and model building were conducted in COOT with subsequent refinement in PHENIX, which included rounds of positional, real-space, *B* factor, and simulated annealing refinement. The use of noncrystallographic symmetry restraints between protomers and the optimization of target weights for geometry and *B* factor restraints greatly improved model quality and refinement statistics. Model building and refinement were continued iteratively until satisfactory statistics were achieved (Tables S1–S6 of the Supporting Information). Water molecules, ions, and any bound substrate were added at the late stages of refinement after the protein portion was deemed to fit satisfactorily. Each KtzI protein structure begins at Pro10 of the wild-type sequence (Figure S1 of the Supporting Information) and ends at residue 423 or 424 (of 424), as residues N- or C-terminal to these positions, respectively, lack electron density and are therefore not included in the final model (Table S7 of the Supporting Information). Residues that lacked clear electron density for their amino acid side chain are modeled as alanines (Table S7 of the Supporting Information). Simulated annealing composite omit maps calculated in PHENIX were used to verify all final models, and each model was inspected and altered to satisfy qualifications set forth by the PDB Validation server.

For structures crystallized under conditions that included NaBr, all ionlike densities were filled exclusively with bromide ions due to (1) the high concentration of bromide used in crystallization (>1.0 M NaBr) compared to the concentrations of other likely ions (e.g., ~0.08 M Cl^-) and (2) the fact that all of these ionlike densities disappeared when KSCN was substituted for NaBr in the crystallization precipitant. It is common for halide ions, like bromide, to compete with water molecules for hydrogen bonding sites, as well as to occupy the solvent shell in and around the protein, and these ions are frequently not at full occupancy.[44] To determine the most representative *B* factor/occupancy combination for the bromide ions, the *B* factor of each was set to the average *B* factor of the late-stage refined model, while the occupancies were set to 0.8, 0.5, and 0.3 in three separate trials. These models were then subjected to 20 rounds of iterative *B* factor and occupancy refinement in PHENIX and found to all converge to the same values, which are those denoted in the final PDB files.

All software installation support was provided by SBGrid.[45] Sequence alignments were completed using Clustal Omega.[46] Structural figures and movies were prepared using PyMOL[47] and Chimera[48] [Chimera is developed by the Resource for Biocomputing, Visualization, and Informatics at the University of California, San Francisco (supported by National Institute of General Medical Sciences Grant P41-GM103311)]. Protein surface area calculations were conducted using the 'Protein interfaces, surfaces and assemblies' service PISA at the European Bioinformatics Institute (http://www.ebi.ac.uk/pdbe/prot_int/pistart.html).[49] All root-mean-square deviation (rmsd) calculations were conducted for Cα atoms only using the Protein structure comparison service Fold at the European Bioinformatics Institute (http://www.ebi.ac.uk/msd-srv/ssm),[50] with a comprehensive list of rmsd comparisons available in Table S8 of the Supporting Information.

RESULTS

The L-ornithine (L-Orn) *N*-hydroxylase from *Kutzneria* sp. 744, KtzI, was structurally characterized by X-ray crystallography, yielding a total of six different snapshots of the enzyme under various conditions (Table 1). The initial structure of KtzI was obtained by reconstituting the purified protein with FAD and NADPH in an anaerobic environment, followed by crystallization under conditions that included NaBr. This structure, and all other structures herein, is abbreviated to signify the molecules to which KtzI is bound and the presumed redox state of its cofactors. Thus, the initial structure of this enzyme is denoted KtzI–FADred–$NADP^+$–Br, as it binds reduced FAD as evidenced by its colorless appearance (Figure S2a of the Supporting Information), oxidized $NADP^+$ due to the hydride transfer necessary to create the FADred species, and a bromide ion in the substrate binding pocket. This structure was determined to 2.4 Å resolution by molecular replacement using the protein coordinates from the functional homologue of KtzI from *P. aeruginosa*, PvdA (PDB entry 3S5W[30]). Two additional structures under conditions that included NaBr were obtained when the enzyme was reconstituted with FAD and NADPH aerobically and then either kept aerobic throughout (KtzI–FADox–Br, 2.1 Å) or re-reduced after crystal growth with sodium dithionite under anaerobic conditions (KtzI–FADox-red–$NADP^+$–Br, 2.6 Å). The oxidized flavin cofactor (FADox, yellow) is readily visible in the KtzI–FADox–Br crystals (Figure S2b of the Supporting Information), confirming the assignment of its redox state. The transition

dx.doi.org/10.1021/bi500655q | *Biochemistry* 2014, 53, 6063–6077

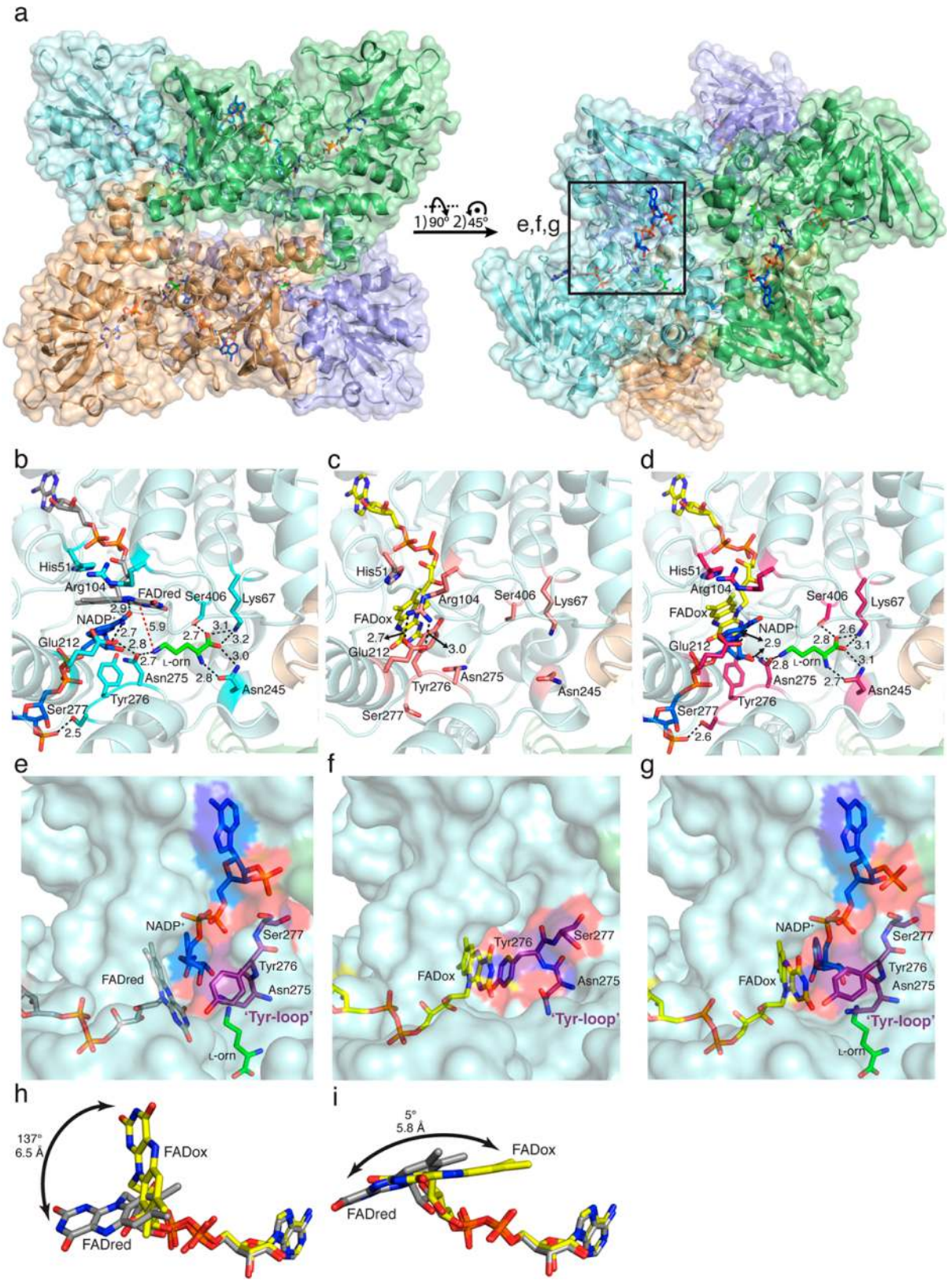

Figure 3. Structure of KtzI in reduced and oxidized states. (a) Overall structure of the KtzI tetramer colored by protomer (pale cyan, pale green, wheat, and pale blue) and represented in ribbons overlaid with a semitransparent surface. (b) Active site of KtzI–FADred–$NADP^+$–L-Orn with FADred, $NADP^+$, and L-Orn (sticks colored gray, marine blue, green, and cyan, respectively) and relevant protein residues displayed. All other atoms are colored as follows: red for oxygen, blue for nitrogen, and orange for phosphorus. Hydrogen bonds are represented as black dashed lines, and a red dashed line shows the distance between the reactive portions of FAD (C4a) and L-Orn (N^5) during hydroxylation (all lengths denoted in angstroms, with arrows used to indicate which distance is associated with each line, if necessary). (c) Active site of KtzI–FADox–Br (aligned by the pale cyan protomer in panel b) showing a large change in conformation from that of its reduced counterpart. FADox and the same active site

dx.doi.org/10.1021/bi500655q | *Biochemistry* 2014, 53, 6063–6077

Figure 3. continued

residues as in panel b are shown as sticks with carbons colored yellow and salmon, respectively. (d) The active site of KtzI–FADox–$NADP^+$–L-Orn is an amalgamation of panels b and c, with $NADP^+$, L-Orn, and active site residues similar to those shown in panel b, and the FAD conformation similar to that in panel c. Active site protein residues are colored dark pink, with all other colors and representations as in panels b and c. (e) One side of the active site of KtzI–FADred–$NADP^+$–L-Orn (shown in surface representation) is capped by $NADP^+$ (colored as in panel b) and a protein loop containing Asn275, Tyr276, and Ser277 (the "Tyr loop", magenta). All other representations and colors are like those in panel b. (f) The surface of the active site shown in panel e changes drastically because of conformational changes and the exit of $NADP^+$. All colors and representations are like those in panel e except the carbons of FADox are colored yellow. (g) The surface represenation of panel d is once again a combination of panels e and f, following the same color scheme. Overlaying the FADred (gray carbons) and FADox (yellow carbons) equilibrium states for both KtzI (h) and *p*-hydroxybenzoate hydroxylase (PHBH) (i) displays the difference between these two proposed conformational changes. The differences in both the angle (degrees) between the isoalloxazine and ribityl tail and the distances (angstroms) from N^5 to N^5 of the isoalloxazine are denoted. Stereoviews for all KtzI structures are shown in Figure S7 of the Supporting Information.

from FADox (yellow) to FADred (colorless) (abbreviated FADox-red) was readily apparent in the dithionite-reduced crystals. It is possible this "re-reduced" structure has NADPH instead of $NADP^+$ bound to the enzyme, because of the chemical reduction by dithionite; however, this cofactor was found to bind in an identical manner to that of its anaerobically reconstituted counterpart, KtzI–FADred–$NADP^+$–Br (as detailed below), and thus, we have named it consistently for the sake of simplicity. It was determined empirically that the condition that included NaBr occluded substrate binding due to a competing bromide ion, and thus, an alternative crystallization precipitant was pursued.

The reconstituted enzyme was found to crystallize using a replacement salt in the precipitant (KSCN), which afforded substrate binding, and three additional structures. Two structures were determined in which KtzI was reconstituted with FAD, NADPH, and L-Orn under anaerobic conditions and then either kept anaerobic (KtzI–FADred–$NADP^+$–L-Orn, 2.2 Å) or allowed to equilibrate with atmospheric oxygen, thus reoxidizing the originally reduced crystals (KtzI–FADred-ox–$NADP^+$–L-Orn, 2.7 Å). The change from colorless [FADred (Figure S2a of the Supporting Information)] to yellow [FADox (Figure S2c of the Supporting Information)] (abbreviated FADred-ox) was used to inform the assignment of the flavin cofactor's redox state. One final structure was determined by following the same reconstitution protocol described above, but under aerobic conditions throughout (KtzI–FADox–$NADP^+$–L-Orn, 2.4 Å), providing off-yellow crystals (Figure S2c of the Supporting Information). These oxidized structures are proposed to bind $NADP^+$ because of this cofactor binding in a conformation that would not (and does not) provide reduction of FAD (detailed below). The protein coordinates from the initial refined model of KtzI (KtzI–FADred–$NADP^+$–Br) were used as a search model in MR or for rigid body refinement to determine all subsequent structures. Data processing and refinement statistics can be found in Tables S1–S6 of the Supporting Information.

Quaternary Structure. Even though KtzI was crystallized under a wide variety of conditions, it was found to adopt the same homotetrameric assembly in each (Figure 3a). Extensive interfaces exist between each of the protomers such that ∼25% of the available surface area is buried by these interactions. These interfaces are conserved in the structures of the KtzI homologues PvdA[30] and SidA,[29] and the same tetramer is generated in these structures by crystal symmetry (Figure S4a of the Supporting Information). The buried surface areas are not quite as extensive for PvdA (17% buried) and SidA (16% buried), largely because of a looser association at one of the interfaces (Figure S4b of the Supporting Information). Although the secondary structure at this interface is similar in all three homologues, the sequence conservation in this region is relatively poor between KtzI and PvdA/SidA [residues 230–235, 260–270, and 325–330 (KtzI numbering) in Figure S1 of the Supporting Information], and the arrangement of residues in KtzI causes a helix to rearrange, yielding a clamping effect (Figure S4b of the Supporting Information). In particular, the aforementioned helix (residues 260–270 in KtzI) moves ∼4–6 Å closer to its adjacent protomer, which allows a cross-protomer hydrogen bond from Tyr270 to the 2′-phosphate of the NADP cofactor (Figure S4b of the Supporting Information). Given that this helix movement is exclusive to KtzI, the monomeric units of SidA and PvdA are more related structurally to one another (rmsd of ∼1.1 Å) than to our enzyme (rmsd of ∼1.4 Å), despite the fact that overall sequence conservation between the proteins is not markedly different (37% identical between SidA and PvdA vs 33% between SidA/PvdA and KtzI). Indeed, the sequence and structural conservation between all three proteins is apparent in the active site.

Active Site of Reduced KtzI. The fully liganded, anaerobic complex of KtzI, KtzI–FADred–$NADP^+$–L-Orn depicts this enzyme in its reduced, "preturnover" state (Figure 2, **4a**, and Figure 3b,e). The FAD and NADP cofactors are bound in an elongated conformation with the nicotinamide of $NADP^+$ stacking on the *re*-face of the flavin isoalloxazine ring. The nicotinamide cofactor is not in a position to reduce the flavin, as its reactive C4 atom is pointed away from the site of reduction (N^5 of the isoalloxazine ring). Instead, the carbonyl oxygen of the nicotinamide is oriented toward this N^5 position by a conserved glutamate residue [Glu212 in KtzI (Figure S1 of the Supporting Information)], allowing the carbonyl oxygen to hydrogen bond with the reduced N^5-H group of FADred (Figure 3b). The flavin isoalloxazine ring is sandwiched between His51 and $NADP^+$ and is found to adopt its bent or butterfly conformation (Figure 3b and Figure S3 of the Supporting Information). There is evidence from structural[51] and computational[52,53] studies that this bend signals the fully reduced state of the cofactor, which would be appropriate in this NADPH-reduced, anaerobic context. However, we find bent isoalloxazine rings in all the structures presented herein, including those from formally oxidized species in which the flavin is surrounded by a completely different protein environment (described in detail below), and thus believe it is unlikely that this phenomenon is chemically or environmentally induced alone. It has been established for the flavin-containing reductase NrdI that interaction with the photoelectrons produced during X-ray exposure can reduce the flavin isoalloxazine ring, generating the bent conformation of the

dx.doi.org/10.1021/bi500655q | *Biochemistry* 2014, 53, 6063–6077

cofactor,[54] and we propose that this is likely to be a contributing factor in our structures, especially those from oxidized preparations.

The amino acid substrate L-Orn is specifically recognized in the active site by hydrogen bonds to its carboxy and amino moieties, as well as to its side chain amine (N^5), by conserved lysine, serine, and asparagine residues [Lys67, Asn245, Asn275, and Ser406 in KtzI (Figure 3b and Figure S1 of the Supporting Information)]. The carbonyl of Asn275 further hydrogen bonds with the 3′-OH of the nicotinamide ribose of $NADP^+$ (Figure 3b). The positioning of L-Orn is such that the site of hydroxylation (N^5) is aligned with the C^{4a} position of the isoalloxazine at a distance (5.9 Å) that would be amenable for catalysis after the addition of oxygen and subsequent creation of the reactive C4a-hydroperoxy intermediate (Figure 3b, red dashed line). This highly reactive center must be protected from bulk solvent, and this role is filled on one side of the active site by the $NADP^+$ cofactor and a protein loop containing Asn275, Tyr276, and Ser277 ["Tyr loop" (Figure 3e)] and on the other by a neighboring protomer (Figure 3b and Figure S4c of the Supporting Information, colored wheat). Removal of these contacts on either side would result in an open active site (Figure 3e and Figure S4c,d of the Supporting Information).

The reduced, preturnover state of KtzI was also crystallized in which the substrate, L-Orn, is replaced with a bromide ion from the precipitant solution (>1.0 M NaBr), and this structure is denoted as KtzI−FADred−$NADP^+$−Br (Figure S5a of the Supporting Information). Even when the compound is reconstituted with a high concentration of L-Orn (31.8 mM), the bromide ion remained bound in the active site, likely because of its vast excess (∼1 M vs 31.8 mM). Bromides were also found to occupy other sites on the protein (Table S2 of the Supporting Information). However, these ions have no real effect on the protein fold (rmsd of 0.3 Å vs KtzI−FADred−$NADP^+$−L-Orn) or on the arrangement of cofactors and crucial active site residues (Figure S5a of the Supporting Information vs Figure 3b).

Active Site of Oxidized KtzI. To obtain a snapshot of E−FADox, KtzI was reconstituted aerobically with FAD and NADPH and then crystallized under conditions that included NaBr (denoted KtzI−FADox−Br). The resulting structure is most different from the other KtzI structures with an rmsd of ∼0.6 Å. This divergence is concentrated in the active site where a drastic structural rearrangement has taken place. In this state, $NADP^+$ has vacated the active site, Arg104 has swung in to hydrogen bond with Glu212, the isoalloxazine ring of FAD has "flapped" completely across the active site, and the Tyr loop has inserted into the active site interior, where Tyr276 stacks with the new conformation of the flavin ring (Figure 3c,f). The absence of bound NADP(H) is quite surprising as a large excess (20-fold vs protein) of NADPH was used during reconstitution. The conformational change from FADred to FADox in KtzI shifts the isoalloxazine ring 6.5 Å (N^5–N^5) and rotates the angle between the flavin ring and its ribityl tail by ∼137° (Figure 3h), which is quite different from the change observed for the prototypic class A flavin hydroxylase, *p*-hydroxybenzoate hydroxylase (PHBH) (Figure 3i). The insertion of the Tyr loop into the active site moves the Cα atom of Tyr276 4.0 Å, such that this residue is now sandwiching the isoalloxazine ring with the help of His51, which has rotated slightly to remain parallel with the flavin cofactor (Figure 3c). The absence of $NADP^+$ and L-Orn has caused other conserved residues (Asn245, Asn275, Ser277, and Ser406) to adopt new conformations with their side chains pointed away from the active site (Figure 3c,f). These drastic rearrangements greatly alter the effective surface of the protein active site, such that the isoalloxazine moiety is now open to solvent (Figure 3f). Aside from this active site reorganization, the rest of the protein topology remains largely the same (rmsd of ∼0.6 Å), with most residues adopting identical conformations. KtzI was also reconstituted aerobically with FAD, NADPH, and L-Orn and crystallized under conditions that included KSCN, which yielded yet another independent snapshot of this state of the enzyme.

Following the same aerobic reconstitution that produced the KtzI−FADox−Br structure, but with the addition of L-Orn and the use of KSCN in place of NaBr, an amalgamation of the fully liganded, anaerobic complex (KtzI−FADred−$NADP^+$−L-Orn) and KtzI−FADox−Br was produced. This structure, denoted as KtzI−FADox−$NADP^+$−L-Orn (Figure 3d,g), is similar to the fully liganded, anaerobic complex, in that it has FAD, $NADP^+$, and L-Orn bound to the protein and the active site residues adopt the same conformation as in the preturnover complex (Figure 3d vs Figure 3b). However, the bound flavin adopts the "flapped" FADox conformation observed in KtzI−FADox−Br (Figure 3d vs Figure 3c). This arrangement appears as if the flavin of the fully liganded anaerobic structure was simply replaced with that of the "flapped", oxidized conformation, such that the $NADP^+$ moiety now stacks with the *si*-face of the isoalloxazine ring (Figure 3d,g).

Both snapshots of the oxidized KtzI enzyme suggest a novel conformational change for a protein-bound flavin molecule; however, they are also quite different from one another (Figure 3c vs Figure 3d). This dissimilarity was quite surprising as the method employed to attain these structures was identical aside from the salt used in the precipitant (NaBr vs KSCN), the resulting absence or presence of a substrate, and a relatively modest change in pH (7.5 vs 8.5). This unanticipated discrepancy, combined with the lack of precedence for either depiction, concerned us that some crystallization artifact may have trapped nonrelevant or dead-end states. In an effort to understand the chemical relevancy of these respective states, manipulations were employed to observe whether the supposed conformational changes could be recapitulated in the protein crystal.

***In Crystallo* Conformational Changes.** In an effort to establish the chemical relevancy of the exposed or "out" position of the FAD observed in the KtzI−FADox−Br structure, crystals were grown as usual and then subjected to chemical reduction by NADPH and sodium dithionite under anaerobic conditions. The crystals showed a definitive color change from yellow (oxidized) to colorless (reduced) when either reductant was used, but structural characterization could be conducted on only the sodium dithionite-reduced crystals. This limitation was due to the fact that a longer incubation period (30 min) was required to fully reduce crystals with NADPH as compared to sodium dithionite (<10 s), and this longer time frame left the crystal too deteriorated for useful data collection.

Amazingly, soaking the oxidized, KtzI−FADox−Br crystals with sodium dithionite under anaerobic conditions provided a structure, denoted as KtzI−FADox-red−$NADP^+$−Br, which is identical (rmsd of 0.15 Å) to that of its anaerobically reconstituted counterpart (KtzI−FADred−$NADP^+$−Br) (Figure S5d vs Figure S5a of the Supporting Information). This finding means that the conformational changes necessary to

dx.doi.org/10.1021/bi500655q | *Biochemistry* 2014, 53, 6063−6077

turn KtzI–FADox–Br into its reduced and NADP-bound species, that is the "flapping" of its isoalloxazine ring across the active site with concomitant evacuation of the Tyr loop and rebinding of the $NADP^+$ cofactor, could all occur in the crystal.

In KtzI–FADox–$NADP^+$–L-Orn, the "flapped", FADox conformation is observed such that the isoalloxazine faces the protein exterior, but $NADP^+$, L-Orn, and all active site residues appear as in the fully liganded anaerobic complex, creating the effect of an $NADP^+$ cofactor slipping behind the "flapped" flavin conformation (Figure 3d,g). Attempts to reduce these crystals, even upon long incubations with NADPH or dithionite, proved futile as no change in color was observed. However, we examined whether the opposite chemical transformation could occur in the crystal, that is from the fully reduced, anaerobic species (Figure 3b) to its oxidized counterpart (Figure 3d), through the addition of oxygen.

Crystals of the KtzI–FADred–$NADP^+$–L-Orn complex were grown anaerobically and then equilibrated aerobically, allowing the flavin cofactor to oxidize. This reoxidized structure (denoted KtzI–FADred-ox–$NADP^+$–L-Orn) is identical (rmsd of 0.13 Å) to that of the aerobically grown, KtzI–FADox–$NADP^+$–L-Orn state (Figure S6b of the Supporting Information vs Figure 3d). Excitingly, this observation means that upon addition of oxygen to the fully liganded, anaerobic complex (Figure 3b), the FAD isoalloxazine was able to travel across the active site from its FADred state to arrive at the FADox position observed in the aerobically reconstituted KtzI structures (Figure 3d,g,h), all while contained in the crystal lattice. Clashing of the FAD and NADP cofactors would likely occur in any FADred to FADox conformational change in KtzI, and thus, the nicotinamide cofactor would be expected to depart during this reoxidation process, signaling that more dynamic changes take place between the equilibrium states than we have observed crystallographically.

DISCUSSION

The flavin-dependent *N*-hydroxylases make up a class of enzymes that have been studied almost exclusively in the context of their role in generating iron-chelating siderophores.[12−23] Here we investigate the L-Orn-specific *N*-monooxygenase from *Kutzneria* sp. 744, KtzI, which instead provides a building block for the biosynthesis of a new class of antifungal antimicrobials called kutznerides[7] (Figure 1a). Regardless of their cellular function, *N*-hydroxylases all catalyze the same reaction, using FAD, NAD(P)H, and molecular oxygen to attach a hydroxyl group on the primary amino side chain of their substrate (Figure 1b). Further, the L-Orn *N*-hydroxylases from *P. aeruginosa* (PvdA) and *A. fumigatus* (SidA), which have sequences highly homologous with that of KtzI (Figure S1 of the Supporting Information), have been observed to follow a common kinetic mechanism[15−17] (Figure 2). Preliminary structural interpretation of this kinetic mechanism has been made possible by recent crystal structures of PvdA[30] and SidA.[29] In this work, we have used KtzI to add to the structural reaction coordinate and provide analogous as well as novel depictions of this enzyme class.

The anaerobically reduced KtzI–FADred–$NADP^+$–L-Orn structure (Figure 3b,e) and an accompanying depiction in which a bromide ion from crystallization has displaced the substrate [KtzI–FADred–$NADP^+$–Br (Figure S5a of the Supporting Information)] are very similar to the aerobically reduced depictions of PvdA[30] (Figure S5b of the Supporting Information) and SidA[29] (Figure S5c of the Supporting Information). This similarity indicates that reconstituting the enzyme in the absence of oxygen, as was done for KtzI, can be approximated by chemical reduction of the aerobic state, and thus, these structures can all be taken together as independent validations of the preturnover state of enzymes in this family. In this state, NADPH has already transferred its hydride to the FAD moiety (Figure 2, **2** → **3**), such that FADred, $NADP^+$, and the L-Orn substrate (or competing bromide ion) are bound in the active site. This redox assignment can be confirmed by the bleached appearance of these crystals (Figure S2a of the Supporting Information), and the fact that the reactive C4 position of the nicotinamide moiety is pointed away from the site of reduction [N^5 of FAD (Figure 3b)] and thus is not positioned for hydride transfer. A conserved glutamate residue [Glu212 in KtzI (Figure S1 of the Supporting Information)] instead poses the nicotinamide such that its carbonyl oxygen can hydrogen bond with the newly formed N^5-H group of reduced flavin (Figure 3b). The bound $NADP^+$ also makes up a large portion of the protein surface (Figure 3e), effectively sealing the active site with its presence. Therefore, in addition to its role in flavin reduction, this cofactor acts to shield the FADred and FAD-OO(H) intermediates (Figure 2, **3**−**5**) from bulk solvent, protecting these species from being quenched. Indeed, there is kinetic evidence from PvdA[30] and SidA[15,16] that $NADP^+$ remains bound throughout the reaction cycle to perform this role. This protective function is further exemplified by the observation that chemical reduction of SidA, followed by exposure to oxygen in the absence of $NADP^+$, resulted in immediate uncoupling through H_2O_2 production[15] (Figure 2, uncoupling), whereas the reactive C4a-(hydro)peroxy intermediate is stabilized (in the absence of its hydroxylatable target) by $NADP^+$ on the order of minutes in both SidA[15,16] and PvdA.[17] There is evidence from kinetic isotope effects and computational studies to suggest the 2′-OH of the ribose of $NADP^+$ may be directly responsible for stabilizing the flavin–peroxide intermediate and, further, may act as the proton donor for creation of the C4a-hydroperoxy derivative.[26] When all these studies are taken together, it is readily apparent that the nicotinamide cofactor is crucial to the entirety of the reaction cycle, well beyond its initial task of reducing the flavin moiety, and this multifaceted involvement is, indeed, a hallmark of the class B monooxygenase family.[32]

The *N*-hydroxylase protein scaffold acts as an additional barrier to species that could quench reactive flavin intermediates. On one side of the active site, the Tyr loop (Tyr276 in KtzI, Tyr285 in PvdA, and Tyr324 in SidA) appears to play a protective role, and on the other, the tetrameric interface blocks solvent access. As was mentioned for the structure of PvdA,[30] if one considers only the monomeric unit of an *N*-hydroxylase, it is difficult to explain the stabilization of the flavin–hydroperoxide intermediate in the absence of L-Orn, because in its absence, the active site is open to solvent (Figure S4d of the Supporting Information). This concern is alleviated, however, by thinking of the protein in terms of the tetrameric assembly observed crystallographically (Figure S4a of the Supporting Information). The interfaces of this tetramer are quite extensive in all three homologues, burying 16−25% of the available surface area, and one of these interfaces guards the active site with its interaction (Figure 3b and Figure S4c of the Supporting Information, wheat-colored protomer). A tetramer is also consistent with gel filtration chromatography data collected on SidA and PvdA,[16,21] alluding to the relevance of this species in solution. Therefore, it can be reasoned that the *N*-hydroxylase

dx.doi.org/10.1021/bi500655q | *Biochemistry* 2014, 53, 6063−6077

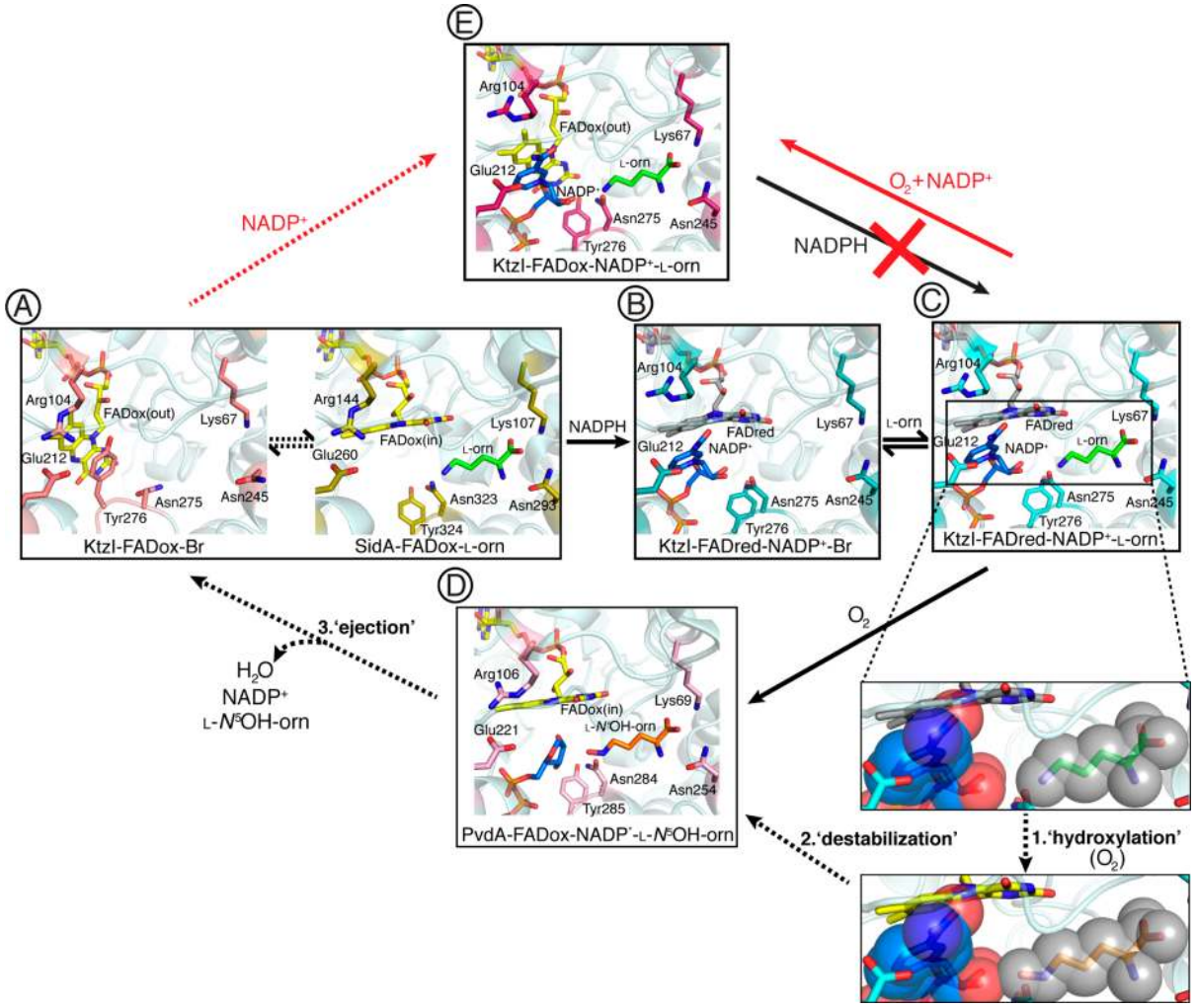

Figure 4. Structurally based proposal for the L-Orn *N*-hydroxylase mechanism. (A) L-Orn *N*-hydroxylases with an oxidized flavin likely exist in a dynamic equilibrium between the FADox(out) conformation observed in KtzI–FADox–Br (with or without the Tyr loop insertion) and the FADox(in) conformation of SidA–FADox–L-Orn (protein carbons colored gold, PDB entry 4B69[29]). (B) Anaerobic reduction of KtzI–FADox–Br crystals recapitulated its anaerobically reconstituted counterpart, KtzI–FADred–$NADP^+$–Br (protein carbons colored teal). (C) Binding of L-Orn, as displayed for KtzI–FADred–$NADP^+$–L-Orn, causes minimal deviations within the active site of the reduced enzyme. A close-up of the active site (inset) with van der Waals radii displayed for substrate L-Orn (gray spheres) and $NADP^+$ (atom-colored spheres) shows the fit of these two molecules. After oxygen addition and hydroperoxy-flavin generation, hydroxylation to the L-N^5OH-Orn product would occur (1). If this newly hydroxylated product (orange carbons) maintains the same positioning as the substrate, a steric clash between the van der Waals radii of the newly added N^5-OH group (gray spheres) and the bound NADP cofactor would occur, which could lead to a destabilization of $NADP^+$ binding (2). (C) This destabilization could explain the poorly resolved nicotinamide portion of $NADP^+$ found in the L-N^5OH-Orn-bound structure of PvdA (PDB entry 3S5W[30]). After catalysis, the resting state enzyme would need to be reproduced through dissociation of the hydroxyornithine product, spent $NADP^+$ cofactor, and water (3). We have shown that a conformational change takes place *in crystallo* after the addition of oxygen to the fully liganded reduced state in panel C, in a background of excess NADP(H), yielding the KtzI–FADox–$NADP^+$–L-Orn state shown in panel E. Crystals of this oxidized state are unable to be reduced by NADPH or dithionite, and thus, it appears to be a dead-end, inhibited conformation. Binding of $NADP^+$ to the FADox(out) state in panel A could cause a state similar to what we observe in panel E, which could be blocked by insertion of the Tyr loop. Dotted line arrows are shown for steps without direct experimental evidence. Colors for protein, cofactors, and ligands not described above are the same as those in Figure 3. Bromide ions were removed from the KtzI structures for the sake of clarity.

tetramer is formed for the protection of reactive intermediates and thus is vital for catalysis. These enzymes, like those of the "cautious" monooxygenase family, also manage catalytic specificity for their L-Orn substrate, and this task is accomplished using a highly organized active site.

L-Orn is secured in the binding pocket by hydrogen bonds made from conserved residues to all of its polar groups (Figure 3b and Figure S1 of the Supporting Information). As was shown in crystal structures of SidA, however, this site is also able to accommodate L-Lys and L-Arg in a highly similar binding mode.[29] There is some evidence that SidA can hydroxylate L-Lys to a certain degree,[29] but studies have mostly found L-Orn *N*-hydroxylases to be highly specific for L-Orn;[7,16,20,21,24] it is thus somewhat surprising to find non-substrates binding in the active site. This discordance seems to indicate that although different L-amino acids can bind similarly to L-Orn, hydroxylation is controlled by the angle and proximity of the amine group to the flavin-hydroperoxide intermediate, such that L-Orn represents the only species in prime position for catalysis. The inability of the L-Orn *N*-monooxygenases to hydroxyate L-lys effectively, with the large amount of uncoupling observed in the presence of this amino

dx.doi.org/10.1021/bi500655q | *Biochemistry* 2014, 53, 6063–6077

acid, indicates that the extra methlyene unit of this molecule extends its amine side chain too far into the active site for hydroxylation to occur but resembles L-Orn enough to trigger oxidative uncoupling (Figure 2, uncoupling). Further insight into the oxidative half of the reaction is provided by our aerobic structures of KtzI.

In contrast to the reduced preturnover states, for which KtzI (Figure 3b and Figure S5a of the Supporting Information), PvdA (Figure S5b of the Supporting Information), and SidA (Figure S5c of the Supporting Information) all show very similar structures, the oxidized structures of KtzI show an unprecedented flavin conformation, which we term the FADox(out) conformation. This "out" conformation shifts the isoalloxazine moiety completely across the active site, such that it is now open to solvent (Figure 3f,g). In KtzI–FADox–Br, the new flavin conformation is accompanied by the dissociation of $NADP^+$, and the movement of conserved active site residues, including insertion of the Tyr loop (Asn275, Tyr276, and Ser277), and swinging of Arg104 such that it takes the place of $NADP^+$ by hydrogen bonding with Glu212 (Figure 3c vs Figure 3b). In KtzI–FADox–$NADP^+$–L-Orn, the "flapped" flavin resides in an active site that is largely unchanged compared to the preturnover complex, with $NADP^+$, L-Orn, and protein residues all adopting similar conformations (Figure 3d vs Figure 3b). In contrast to both of the KtzI–FADox structures, the structure of the FADox state of SidA shows FAD in the "in" position with substrate bound and no $NADP^+$ [Figure 4, A (right)[29]]. Interestingly, the hydrogen bond switch from Glu212-$NADP^+$ (Figure 3b) to Glu212-Arg104 (Figure 3c) observed in KtzI was also observed in the crystal structures of reduced versus oxidized states of SidA [Figure S5c of the Supporting Information vs Figure 4, A (right)].

Given the novelty of this "out" FAD conformation in KtzI, it was important to establish the chemical competence of this flavin position, and we found that the FADox(out) state observed in the KtzI–FADox–Br structure is, in fact, chemically competent. Specifically, KtzI–FADox–Br crystals subjected to anaerobic reduction by NADPH (50 mM) and sodium dithionite (25 mM) visibly changed from yellow (Figure S2b of the Supporting Information) to colorless (Figure S2a of the Supporting Information), and the conformation of the active site returned to its reduced preturnover state *in crystallo* (Figure S5d vs Figure S5a of the Supporting Information; rmsd = 0.15 Å). Sodium dithionite could be acting as a conduit for NADPH reduction of FADox, as its low reduction potential allows it to reduce the leftover $NADP^+$ in the crystallization drop (which then goes on to reduce FADox) or it could be reducing the FADox directly. In any case, the recapitulation of the reduced, preturnover state from this oxidized state using chemical means provides compelling evidence of the chemical competence of this transformation. Regrettably, structural data contain no information about reaction rates, so catalytic relevance can be only inferred, and not directly measured.

In contrast to facile reduction of KtzI–FADox–Br crystals, KtzI–FADox–$NADP^+$–L-Orn crystals could not be reduced. No change in color was observed upon addition of NADPH or sodium dithionite, and no structural changes were observed in characterized crystals (data not shown). This result suggests that when FAD movement is blocked by the binding of excess $NADP^+$ and L-Orn, FAD reduction does not occur. Because the amounts of $NADP^+$ and L-Orn used in these crystallization studies are above physiological concentrations, this inhibition observed *in crystallo* is unlikely to be relevant *in vivo*. Thus, our crystallographic studies show that when the FAD is free to flap, movement from "out" to "in" accompanies flavin reduction in the crystal.

Further support for motions being involved in KtzI catalysis comes from the *in crystallo* reoxidation of the fully liganded, anaerobic state. KtzI–FADred–$NADP^+$–L-Orn crystals (Figure 3b,e) equilibrated in atmospheric oxygen generated the KtzI–FADred-ox–$NADP^+$–L-Orn structure, which fully recapitulates the structure of its aerobically reconstituted counterpart (Figure S6b of the Supporting Information vs Figure 3d; rmsd = 0.13 Å). Impressively, the enzyme used to obtain the KtzI–FADred-ox–$NADP^+$–L-Orn structure underwent multiple transformations, from aerobic solution to anaerobic reduction by NADPH to anaerobic crystallization to air oxidation of the crystal. The snapshot we see is the end product of these motions. Indeed, via comparison of the structures before (Figure 3b) and after (Figure S6b of the Supporting Information) oxygen exposure, it becomes apparent that any movement of the flavin moiety to get from the FADred to FADox(out) conformation would be sterically occluded by the bound $NADP^+$. In other words, intermediate states must exist in which $NADP^+$ dissociates, the flavin moves, and $NADP^+$ reassociates. Further, the L-Orn bound in this structure is certainly not the same as the L-Orn bound initially, which would be expected to have been hydroxylated upon exposure of the fully loaded, preturnover enzyme to O_2 but instead represents another molecule that has rebound sometime during the reoxidation process. These rebinding events are likely driven by the excess amounts of both NADP(H) and L-Orn left in the crystallization drop, which remain present during reoxidation of the crystals. Whether these conformational changes between equilibrium states occur multiple times cannot be discerned from our studies; however, our data show that they must occur at least once. It is interesting that movement of FADox(out) to FADred(in) cannot occur in the presence of bound $NADP^+$ and L-Orn (KtzI–FADox–$NADP^+$–L-Orn crystals cannot be reduced), but movement from FADred(in) to FADox(out) can occur (the KtzI–FADred-ox–$NADP^+$–L-Orn result). These results raise the very important question of the mechanistic role of this conformational change of FAD.

A conformational change in a flavin-dependent hydroxylase is not a new observation. Indeed, "cautious" monooxygenases control faithful coupling of NADPH reduction to substrate hydroxylation by movements of their flavin moiety (reviewed in refs 31 and 32). As mentioned previously, "cautious" (or class A) monooxygenases get their name from the fact that in these enzymes, NADPH will reduce FAD only when substrate is bound, thus limiting oxidative uncoupling (Figure 2, uncoupling). The structural basis for this phenomenon was first proposed for *p*-hydroxybenzoate hydroxylase (PHBH),[55] where substrate-coupled reduction is controlled by a planar, hingelike movement of the FAD isoalloxazine ring from the protein interior ("in") to the protein exterior ("out") upon substrate binding (Figure 3i), which allows NADPH access to reduce FADox. Once reduction occurs, the flavin moves from this "out" position back "in" to protect its reduced N^5-H group from solvent. Although this precedence exists for "cautious" enzymes, KtzI is the first class B monooxygenase proposed to use flavin conformational changes during catalysis, and these movements are even more drastic than those of the class A systems (Figure 3h vs Figure 3i).

We know the conformational changes observed for KtzI are not correlated in the same way as "cautious" enzymes, as L-Orn *N*-hydroxylases, like "bold" monooxygenases, can just as easily be reduced in the absence of substrate. Further, oxidized SidA and PvdA crystals (whose structures resemble those seen for the reduced KtzI states) were reduced *in crystallo* without any indication of a conformational change,[29,30] so the flavin does not necessarily need to start in an "out" position for reduction to occur. To formulate the mechanistic implications of these conformational changes, it is pertinent to consider another trait *N*-hydroxylases share with "bold" monooxygenases; that is, $NADP^+$ remains bound throughout the reaction cycle and, thus, dissociates only after hydroxylation occurs. This observation means that there must be some signal for $NADP^+$ to dissociate, such that another round of catalysis can occur. By combining our snapshots of KtzI with those of PvdA and SidA, we believe a structural reaction coordinate for *N*-hydroxylase enzymes (summarized in Figure 4 and Movie 1 of the Supporting Information) can be built that utilizes conformational changes to control catalysis, which may provide further insight into the "bold" monooxygenase family in general.

L-Orn *N*-hydroxylases in their resting, oxidized flavin state seem to exist in an equilibrium between the FADox(out) conformation observed in KtzI–FADox–Br (with or without insertion of the conserved Tyr loop), and the FADox(in) conformation of SidA–FADox–L-Orn (Figure 4, A). NADPH then reduces FADox, but the exact orientation of NADPH to FAD that is responsible for reduction has not been captured in any of the KtzI, SidA, or PvdA structures; only the postreduction conformation of $NADP^+$ is observed. A so-called "sliding mechanism" for NADPH reduction has been suggested for the Baeyer–Villiger monooxygenase (BVMO) class of "bold" monooxygenases, in which the nicotinamide adopts different conformations during and after reduction. This proposal is largely based on the observation of varied binding modes of this cofactor in crystal structures,[56,57] and the indication from kinetic studies that the reduction process happens in two phases, one of which is consistent with an equilibration step for NADPH in the binding pocket.[58] The sliding mechanism has also been proposed for SidA,[25] as biphasic reduction kinetics have been observed for both PvdA[17] and SidA,[15,27] and there is evidence from a mutant of SidA (Ser257Ala) that destabilizing a hydrogen bonding interaction to the pyrophosphate of $NADP^+$ actually increases the reduction rate, suggesting that a more dynamic nicotinamide ring is favorable for this step.[25] Although our data do not provide further information about this sliding mechanism directly, the FADox(out) conformation we observe, and have shown to at least be chemically competent, adds an extra layer to consider when thinking about the reduction step. Indeed, the FADox(out) conformation may contribute to the complicated kinetics of reduction observed for these enzymes.

After $NADP^+$ binding and FAD reduction, conserved residues have been observed to rearrange in both KtzI (Figure 4, A → B) and SidA [Figure 4, A (right) vs Figure S5c of the Supporting Information], such that Arg104 (Arg144) swings out of the $NADP^+$ binding pocket, allowing Glu212 (Glu260) to hydrogen bond to the carboxamide of $NADP^+$, orienting this cofactor to protect the N^5-H group of FADred. Binding of L-Orn to the preturnover, anaerobic state (Figure 4, B → C) causes only minor rearrangements of substrate-binding residues (Lys67, Asn245, and Ser406), as our structures with bromide or substrate bound in this site are very similar (rmsd = 0.3 Å), and those of SidA without substrate bound look largely similar.[29] The addition of molecular oxygen to this preturnover state, regardless of whether the substrate is bound, creates the reactive hydroperoxy-flavin. This transformation is also unlikely to cause any structural deviations, as the binding affinity for L-Orn has been shown to be similar in the reduced versus hydroperoxide-flavin forms of SidA,[15] and $NADP^+$ remains bound to both states,[15−17] suggesting a similar active site architecture. Once the hydroxyl group is picked up by L-Orn, however, the enzyme must be recycled to its resting state in some way.

The hydroxylation step immediately precedes the departure of $NADP^+$ in biochemical studies,[15,16,30] and the structural transmission of this signal may be exemplified by the post-turnover structure of PvdA [PvdA–FADox–$NADP^+$–L-N^5OH-Orn (Figure 4, D)]. In this structure, aerobic reconstitution of PvdA with FAD, NADPH, and L-Orn (turnover conditions), followed by crystallization, trapped the product complex in the crystal. The electron density for the nicotinamide of $NADP^+$ is disordered in this state, such that this cofactor could not be modeled effectively, indicating this moiety is dynamic in the product-bound state.[30] We propose that the act of taking L-Orn [Figure 4, C (inset)] to L-N^5OH-Orn (Figure 4, 1 "hydroxylation") causes a steric clash with $NADP^+$, which propagates to destabilize this cofactor (Figure 4, 2 "destabilization"). The destabilization of $NADP^+$ was not enough, however, to actually dissociate this spent cofactor, as it remains bound in the PvdA structure (Figure 4, D). The lack of a clear departure signal allows us to propose that for $NADP^+$ to leave, the flavin conformational change from the FADox(in) to FADox(out) state that we observe for KtzI is used to eject the oxidized nicotinamide cofactor in the last step of catalysis (Figure 4, 3 "ejection"). During an interpolation between these two conformations, $NADP^+$ and FAD would clash directly, and thus, FAD could act as a steric battering ram to eject $NADP^+$ from the active site. This would not be the first time that a flavin has been proposed to act in a steric capacity, as we recently proposed from structural and biochemical studies of the FAD-dependent hydroxylase StaC, that this class A enzyme uses the "in" movement of its flavin moiety to sterically induce decarboxylation of its substrate molecule.[59] As mentioned above, $NADP^+$ ejection has been linked to the last step in the catalytic cycle of both PvdA[30] and SidA[15,16] by kinetic studies, and the difficulty in deconvoluting the spectra for this oxidative process in SidA[15] hints that something more complex than mere dissociation of $NADP^+$ may occur. Therefore, with all the evidence presented for KtzI, a case has been made for the "flapping" of the flavin moiety to be an integral part of the catalytic cycle.

In addition to revealing on-pathway states, crystallography has also shown us off-pathway conformations. The flavin moiety in the FADox(out)–$NADP^+$ bound conformation (Figure 4, E) could not be reduced by sodium dithionite or NADPH, indicating that the binding of $NADP^+$ behind the FADox(out) conformation inhibits this reduction step (Figure 4, E → C). Indeed, reduction of the flavin, without subsequent movement inside the protein, would only be transient in nature as it is completely solvent-exposed (Figure 3g), which leaves it unprotected from uncoupling upon exposure to oxygen. This observation allows us to propose that $NADP^+$ is inhibiting reduction by blocking the conformational change from FADox(out) to the "in" position of FADred (Figure 4, E → C). Further, insertion of the Tyr loop, as seen for KtzI–

FADox−Br [Figure 4, A (left)], could function to disfavor rebinding of $NADP^+$, guarding against this dead-end, inhibited state under physiological conditions. We could also reach this dead-end, FADox(out)−$NADP^+$ bound state (Figure 4, E) by exposure of the preturnover, anaerobic state to oxygen (Figure 4, C → E), demonstrating that the "in" to "out" movement of FAD necessary to eject $NADP^+$ is chemically accessible *in crystallo*. Taken together (Figure 4), structures of KtzI, SidA, and PvdA have painted a portrait of the reaction coordinate of L-Orn *N*-hydroxylases. A visual synopsis is shown in Movie 1 of the Supporting Information.

In summary, we have observed drastic differences in the active site of a flavin-dependent *N*-hydroxylase through a series of crystallographic snapshots. On the basis of these snapshots, we propose that KtzI, and other *N*-hydroxylases, will use a "flapping" flavin to help eject spent $NADP^+$ from their active sites following turnover, providing a molecular explanation for how these enzymes reset for the next round of catalysis. Considering that the mechanism for $NADP^+$ ejection has been enigmatic for all class B monooxygenases, it is tempting to speculate that flavin conformational changes could also be involved. Before this work, mobile flavins were only associated with PHBH-like "cautious" enzymes, whereas now we find flavin movement in an enzyme that is best defined as a "bold" monoxygenase. Although the trigger for flavin movement appears different in these two distinct enzyme classes, in both cases, the flavin movement appears to be associated with a strategy for preventing uncoupling of the reductive and oxidative half-reactions. We hope that our structural observations will provide a new lens for further biochemical examination of these interesting flavoenzymes.

■ ASSOCIATED CONTENT

Supporting Information

Crystallographic data collection and refinement statistics (Tables S1−S6), a list of ordered residues in crystal structures (Table S7), rmsd comparisons for all structures (Table S8), a sequence alignment of the structurally characterized L-Orn *N*-hydroxylases (Figure S1), representative crystals of KtzI (Figure S2), additional figures of crystal structures (Figures S3−S7), and a movie summarizing our proposal for the conformational dynamics accessible during catalysis (Movie 1). This material is available free of charge via the Internet at http://pubs.acs.org.

Accession Codes

The atomic coordinates have been deposited in the Protein Data Bank as entries 4TLX, 4TLZ, 4TM0, 4TM1, 4TM3, and 4TM4.

■ AUTHOR INFORMATION

Corresponding Author

*E-mail: cdrennan@mit.edu. Telephone: (617) 253-5622. Fax: (617) 258-7847.

Present Address

⊥J.R.H.: Department of Chemistry, University of Utah, 315 S. 1400 E., Salt Lake City, UT 84112-0850.

Funding

This work was supported, in part, by National Institutes of Health Grants GM083464 (to J.R.H.) and GM020011 (to C.T.W.). C.L.D. is an investigator of The Howard Hughes Medical Institute. This work is based upon research conducted at the Advanced Photon Source on the Northeastern Collaborative Access Team beamlines, which are supported by Award RR-15301 from the National Center for Research Resources. Use of the Advanced Photon Source, an Office of Science User Facility operated for the U.S. Department of Energy (DOE) Office of Science by Argonne National Laboratory, was supported by the U.S. DOE under Contract DE-AC02-06CH11357. Financial support comes principally from the Offices of Biological and Environmental Research and of Basic Energy Sciences of the U.S. DOE, the National Center for Research Resources (P41RR012408), and the National Institute of General Medical Sciences (P41GM103473).

Notes

The authors declare no competing financial interest.

■ ACKNOWLEDGMENTS

We thank Yimin Zhao for assisting with crystallization experiments.

■ ABBREVIATIONS

NRPS, nonribosomal peptide synthesis; L-Orn, L-ornithine; KtzI, L-Orn *N*-hydroxylase from *Kutzneria* sp. 744; PvdA, L-Orn *N*-hydroxylase from *P. aeruginosa*; SidA, L-Orn *N*-hydroxylase from *A. fumigatus*; PHBH, *p*-hydroxybenzoate hydroxylase; BVMO, Baeyer−Villiger monooxygenase; FMO, flavin monooxygenase; PEG, polyethylene glycol; PDB, Protein Data Bank; MR, molecular replacement; FADred, reduced FAD; FADox, oxidized FAD; FADox-red, re-reduced FAD; FADred-ox, reoxidized FAD; rmsd, root-mean-square deviation.

■ REFERENCES

(1) Newman, D. J., and Cragg, G. M. (2012) Natural products as sources of new drugs over the 30 years from 1981 to 2010. *J. Nat. Prod. 75*, 311−335.

(2) Walsh, C. T., and Wencewicz, T. A. (2013) Prospects for new antibiotics: A molecule-centered perspective. *J. Antibiot. 67*, 7−22.

(3) Pohanka, A., Menkis, A., Levenfors, J., and Broberg, A. (2006) Low-abundance kutznerides from *Kutzneria* sp. 744. *J. Nat. Prod. 69*, 1776−1781.

(4) Broberg, A., Menkis, A., and Vasiliauskas, R. (2006) Kutznerides 1−4, depsipeptides from the actinomycete *Kutzneria* sp. 744 inhabiting mycorrhizal roots of *Picea abies* seedlings. *J. Nat. Prod. 69*, 97−102.

(5) Fujimori, D. G., Hrvatin, S., Neumann, C. S., Strieker, M., Marahiel, M. A., and Walsh, C. T. (2007) Cloning and characterization of the biosynthetic gene cluster for kutznerides. *Proc. Natl. Acad. Sci. U.S.A. 104*, 16498−16503.

(6) Zolova, O. E., and Garneau-Tsodikova, S. (2013) KtzJ-dependent serine activation and O-methylation by KtzH for kutznerides biosynthesis. *J. Antibiot. 67*, 59−64.

(7) Neumann, C. S., Jiang, W., Heemstra, J. R., Gontang, E. A., Kolter, R., and Walsh, C. T. (2012) Biosynthesis of Piperazic Acid via N(5)-Hydroxy-Ornithine in *Kutzneria* spp. 744. *ChemBioChem 13*, 972−976.

(8) Jiang, W., Heemstra, J. R., Forseth, R. R., Neumann, C. S., Manaviazar, S., Schroeder, F. C., Hale, K. J., and Walsh, C. T. (2011) Biosynthetic Chlorination of the Piperazate Residue in Kutzneride Biosynthesis by KthP. *Biochemistry 50*, 6063−6072.

(9) Strieker, M., Nolan, E. M., Walsh, C. T., and Marahiel, M. A. (2009) Stereospecific synthesis of threo- and erythro-β-hydroxyglutamic acid during kutzneride biosynthesis. *J. Am. Chem. Soc. 131*, 13523−13530.

(10) Neumann, C. S., and Walsh, C. T. (2008) Biosynthesis of (−)-(1S,2R)-allocoronamic acyl thioester by an Fe(II)-dependent halogenase and a cyclopropane-forming flavoprotein. *J. Am. Chem. Soc. 130*, 14022−14023.

(11) Heemstra, J. R., and Walsh, C. T. (2008) Tandem action of the O_2- and $FADH_2$-dependent halogenases KtzQ and KtzR produce 6,7-

dichlorotryptophan for kutzneride assembly. *J. Am. Chem. Soc. 130*, 14024−14025.
(12) Bosello, M., Mielcarek, A., Giessen, T. W., and Marahiel, M. A. (2012) An enzymatic pathway for the biosynthesis of the formylhydroxyornithine required for rhodochelin iron coordination. *Biochemistry 51*, 3059−3066.
(13) Robinson, R., and Sobrado, P. (2011) Substrate binding modulates the activity of *Mycobacterium smegmatis* G, a flavin-dependent monooxygenase involved in the biosynthesis of hydroxamate-containing siderophores. *Biochemistry 50*, 8489−8496.
(14) Robbel, L., Helmetag, V., Knappe, T. A., and Marahiel, M. A. (2011) Consecutive enzymatic modification of ornithine generates the hydroxamate moieties of the siderophore erythrochelin. *Biochemistry 50*, 6073−6080.
(15) Mayfield, J. A., Frederick, R. E., Streit, B. R., Wencewicz, T. A., Ballou, D. P., and DuBois, J. L. (2010) Comprehensive spectroscopic, steady state, and transient kinetic studies of a representative siderophore-associated flavin monooxygenase. *J. Biol. Chem. 285*, 30375−30388.
(16) Chocklett, S. W., and Sobrado, P. (2010) *Aspergillus fumigatus* SidA is a highly specific ornithine hydroxylase with bound flavin cofactor. *Biochemistry 49*, 6777−6783.
(17) Meneely, K. M., Barr, E. W., Bollinger, J. M., and Lamb, A. L. (2009) Kinetic mechanism of ornithine hydroxylase (PvdA) from *Pseudomonas aeruginosa*: Substrate triggering of O_2 addition but not flavin reduction. *Biochemistry 48*, 4371−4376.
(18) Heemstra, J. R., Walsh, C. T., and Sattely, E. S. (2009) Enzymatic tailoring of ornithine in the biosynthesis of the *Rhizobium* cyclic trihydroxamate siderophore vicibactin. *J. Am. Chem. Soc. 131*, 15317−15329.
(19) Pohlmann, V., and Marahiel, M. A. (2008) Delta-amino group hydroxylation of L-ornithine during coelichelin biosynthesis. *Org. Biomol. Chem. 6*, 1843−1848.
(20) Meneely, K. M., and Lamb, A. L. (2007) Biochemical characterization of a flavin adenine dinucleotide-dependent monooxygenase, ornithine hydroxylase from *Pseudomonas aeruginosa*, suggests a novel reaction mechanism. *Biochemistry 46*, 11930−11937.
(21) Ge, L., and Seah, S. Y. K. (2006) Heterologous expression, purification, and characterization of an L-ornithine N(5)-hydroxylase involved in pyoverdine siderophore biosynthesis in *Pseudomonas aeruginosa*. *J. Bacteriol. 188*, 7205−7210.
(22) Thariath, A. M. A., Fatum, K. L. K., Valvano, M. A. M., and Viswanatha, T. T. (1993) Physico-chemical characterization of a recombinant cytoplasmic form of lysine: N6-Hydroxylase. *Biochim. Biophys. Acta 1203*, 27−35.
(23) Plattner, H. J., Pfefferle, P., Romaguera, A., Waschütza, S., and Diekmann, H. (1989) Isolation and some properties of lysine N6-hydroxylase from *Escherichia coli* strain EN222. *Biol. Met. 2*, 1−5.
(24) Frederick, R. E., Ojha, S., Lamb, A., and DuBois, J. L. (2014) How pH Modulates the Reactivity and Selectivity of a Siderophore-Associated Flavin Monooxygenase. *Biochemistry 53*, 2007−2016.
(25) Shirey, C., Badieyan, S., and Sobrado, P. (2013) Role of Ser-257 in the Sliding Mechanism of NADP(H) in the Reaction Catalyzed by the *Aspergillus fumigatus* Flavin-dependent Ornithine N5-Monooxygenase SidA. *J. Biol. Chem. 288*, 32440−32448.
(26) Robinson, R. M., Badieyan, S., and Sobrado, P. (2013) C4a-hydroperoxyflavin formation in N-hydroxylating flavin monooxygenases is mediated by the 2′-OH of the nicotinamide ribose of $NADP^+$. *Biochemistry 52*, 9089−9092.
(27) Romero, E., Fedkenheuer, M., Chocklett, S. W., Qi, J., Oppenheimer, M., and Sobrado, P. (2012) Dual role of NADP(H) in the reaction of a flavin dependent N-hydroxylating monooxygenase. *Biochim. Biophys. Acta 1824*, 850−857.
(28) Frederick, R. E., Mayfield, J. A., and DuBois, J. L. (2011) Regulated O_2 activation in flavin-dependent monooxygenases. *J. Am. Chem. Soc. 133*, 12338−12341.
(29) Franceschini, S., Fedkenheuer, M., Vogelaar, N. J., Robinson, H. H., Sobrado, P., and Mattevi, A. (2012) Structural insight into the mechanism of oxygen activation and substrate selectivity of flavin-dependent N-hydroxylating monooxygenases. *Biochemistry 51*, 7043−7045.
(30) Olucha, J., Meneely, K. M., Chilton, A. S., and Lamb, A. L. (2011) Two structures of an N-hydroxylating flavoprotein monooxygenase: Ornithine hydroxylase from *Pseudomonas aeruginosa*. *J. Biol. Chem. 286*, 31789−31798.
(31) Palfey, B. A., and McDonald, C. A. (2010) Control of catalysis in flavin-dependent monooxygenases. *Arch. Biochem. Biophys. 493*, 26−36.
(32) van Berkel, W. J. H., Kamerbeek, N. M., and Fraaije, M. W. (2006) Flavoprotein monooxygenases, a diverse class of oxidative biocatalysts. *J. Biotechnol. 124*, 670−689.
(33) Entsch, B., Cole, L. J., and Ballou, D. P. (2005) Protein dynamics and electrostatics in the function of p-hydroxybenzoate hydroxylase. *Arch. Biochem. Biophys. 433*, 297−311.
(34) Husain, M., and Massey, V. (1979) Kinetic studies on the reaction of p-hydroxybenzoate hydroxylase. Agreement of steady state and rapid reaction data. *J. Biol. Chem. 254*, 6657−6666.
(35) Krueger, S. K., and Williams, D. E. (2005) Mammalian flavin-containing monooxygenases: Structure/function, genetic polymorphisms and role in drug metabolism. *Pharmacol. Ther. 106*, 357−387.
(36) Otwinowski, Z., and Minor, W. (1997) Processing of X-ray diffraction data collected in oscillation mode. *Methods Enzymol. 276*, 307−326.
(37) McCoy, A. J., Grosse-Kunstleve, R. W., Adams, P. D., Winn, M. D., Storoni, L. C., and Read, R. J. (2007) Phaser crystallographic software. *J. Appl. Crystallogr. 40*, 658−674.
(38) Stein, N. (2008) CHAINSAW: A program for mutating pdb files used as templates in molecular replacement. *J. Appl. Crystallogr. 41*, 641−643.
(39) Murshudov, G., Vagin, A., and Dodson, E. (1997) Refinement of macromolecular structures by the maximum-likelihood method. *Acta Crystallogr. D53*, 240−255.
(40) Emsley, P., and Cowtan, K. (2004) Coot: Model-building tools for molecular graphics. *Acta Crystallogr. D60*, 2126−2132.
(41) Vagin, A. A., Steiner, R. A., Lebedev, A. A., Potterton, L., McNicholas, S., Long, F., and Murshudov, G. N. (2004) REFMAC5 dictionary: Organization of prior chemical knowledge and guidelines for its use. *Acta Crystallogr. D60*, 2184−2195.
(42) Moriarty, N. W., Grosse-Kunstleve, R. W., and Adams, P. D. (2009) electronic Ligand Builder and Optimization Workbench (eLBOW): A tool for ligand coordinate and restraint generation. *Acta Crystallogr. D65*, 1074−1080.
(43) Adams, P. D., Afonine, P. V., Bunkoczi, G., Chen, V. B., Davis, I. W., Echols, N., Headd, J. J., Hung, L.-W., Kapral, G. J., Grosse-Kunstleve, R. W., McCoy, A. J., Moriarty, N. W., Oeffner, R., Read, R. J., Richardson, D. C., Richardson, J. S., Terwilliger, T. C., and Zwart, P. H. (2010) PHENIX: A comprehensive Python-based system for macromolecular structure solution. *Acta Crystallogr. D66*, 213−221.
(44) Dauter, Z., Dauter, M., and Rajashankar, K. R. (2000) Novel approach to phasing proteins: Derivatization by short cyro-soaking with halides. *Acta Crystallogr. D56*, 232−237.
(45) Morin, A., Eisenbraun, B., Key, J., Sanschagrin, P. C., Timony, M. A., Ottaviano, M., and Sliz, P. (2013) Cutting edge: Collaboration gets the most out of software. *eLife 2*, e01456.
(46) Sievers, F., Wilm, A., Dineen, D., Gibson, T. J., Karplus, K., Li, W., Lopez, R., McWilliam, H., Remmert, M., Söding, J., Thompson, J. D., and Higgins, D. G. (2011) Fast, scalable generation of high-quality protein multiple sequence alignments using Clustal Omega. *Mol. Syst. Biol. 7*, 539.
(47) *The PyMOL Molecular Graphics System*, version 1.5.0.5 (2010) Schrodinger, LLC, Portland, OR.
(48) Pettersen, E. F., Goddard, T. D., Huang, C. C., Couch, G. S., Greenblatt, D. M., Meng, E. C., and Ferrin, T. E. (2004) UCSF Chimera: A visualization system for exploratory research and analysis. *J. Comput. Chem. 25*, 1605−1612.
(49) Krissinel, E., and Henrick, K. (2007) Inference of macromolecular assemblies from crystalline state. *J. Mol. Biol. 372*, 774−797.

(50) Krissinel, E. E., and Henrick, K. K. (2004) Secondary-structure matching (SSM), a new tool for fast protein structure alignment in three dimensions. *Acta Crystallogr. D60*, 2256−2268.
(51) Lennon, B. W., Williams, C. H., and Ludwig, M. L. (1999) Crystal structure of reduced thioredoxin reductase from *Escherichia coli*: Structural flexibility in the isoalloxazine ring of the flavin adenine dinucleotide cofactor. *Protein Sci. 8*, 2366−2379.
(52) Rodríguez-Otero, J., Martínez-Núñez, E., Peña-Gallego, A., and Vázquez, S. A. (2002) The role of aromaticity in the planarity of lumiflavin. *J. Org. Chem. 67*, 6347−6352.
(53) Zheng, Y. J., and Ornstein, R. L. (1996) A theoretical study of the structures of flavin in different oxidation and protonation states. *J. Am. Chem. Soc. 118*, 9402−9408.
(54) Røhr, A. K., Hersleth, H.-P., and Andersson, K. K. (2010) Tracking flavin conformations in protein crystal structures with Raman spectroscopy and QM/MM calculations. *Angew. Chem. 49*, 2324−2327.
(55) Gatti, D. L., Palfey, B. A., Lah, M. S., Entsch, B., Massey, V., Ballou, D. P., and Ludwig, M. L. (1994) The mobile flavin of 4-OH benzoate hydroxylase. *Science 266*, 110−114.
(56) Mirza, I. A., Yachnin, B. J., Wang, S., Grosse, S., Bergeron, H., Imura, A., Iwaki, H., Hasegawa, Y., Lau, P. C. K., and Berghuis, A. M. (2009) Crystal structures of cyclohexanone monooxygenase reveal complex domain movements and a sliding cofactor. *J. Am. Chem. Soc. 131*, 8848−8854.
(57) Franceschini, S., van Beek, H. L., Pennetta, A., Martinoli, C., Fraaije, M. W., and Mattevi, A. (2012) Exploring the Structural Basis of Substrate Preferences in Baeyer-Villiger Monooxygenases: Insight from Steroid Monooxygenase. *J. Biol. Chem. 287*, 22626−22634.
(58) Sheng, D., Ballou, D. P., and Massey, V. (2001) Mechanistic studies of cyclohexanone monooxygenase: Chemical properties of intermediates involved in catalysis. *Biochemistry 40*, 11156−11167.
(59) Goldman, P. J., Ryan, K. S., Hamill, M. J., Howard-Jones, A. R., Walsh, C. T., Elliott, S. J., and Drennan, C. L. (2012) An unusual role for a mobile flavin in StaC-like indolocarbazole biosynthetic enzymes. *Chem. Biol. 19*, 855−865.